Chemistry & Biology, Vol. 10, 319–329, April, 2003, ©2003 Elsevier Science Ltd. All rights reserved. DOI 10.1016/S1074-5521(03)00070-X

Analysis of the Importance of the Metallo-β-Lactamase Active Site Loop in Substrate Binding and Catalysis

Catherine Moali,[1] Christine Anne,[1] Josette Lamotte-Brasseur,[1] Sylvie Groslambert,[2] Bart Devreese,[3] Jozef Van Beeumen,[3] Moreno Galleni,[1] and Jean-Marie Frère[1,*]

[1]Centre d'Ingénierie des Protéines
[2]Laboratoire de Génie Chimique
Institut de Chimie B6
Université de Liège
Sart-Tilman
B-4000 Liège
[3]Laboratorium voor Eiwitbiochemie
en Eiwitengineering
Universiteit Gent
K.L. Ledeganckstraat 35
B-9000 Gent
Belgium

Summary

The role of the mobile loop comprising residues 60–66 in metallo-β-lactamases has been studied by site-directed mutagenesis, determination of kinetic parameters for six substrates and two inhibitors, pre-steady-state characterization of the interaction with chromogenic nitrocefin, and molecular modeling. The W64A mutation was performed in IMP-1 and BcII (after replacement of the BcII 60–66 peptide by that of IMP-1) and always resulted in increased K_i and K_m and decreased k_{cat}/K_m values, an effect reinforced by complete deletion of the loop. k_{cat} values were, by contrast, much more diversely affected, indicating that the loop does not systematically favor the best relative positioning of substrate and enzyme catalytic groups. The hydrophobic nature of the ligand is also crucial to strong interactions with the loop, since imipenem was almost insensitive to loop modifications.

Introduction

Metallo-β-lactamases have been the subject of growing interest in the past few years due to their increasing occurrence in pathogenic bacterial strains, their rapid dissemination by horizontal transfer, and the lack of efficient therapy to treat infected patients. Since the discovery of the first metallo-β-lactamase in almost innocuous strains of *Bacillus cereus* [1], at least twelve new enzymes have been described, and several variant forms are already known for some of them.

Metallo-β-lactamases (also referred to as class B β-lactamases) use one or two zinc ions as physiological cofactors and are usually capable of hydrolyzing a large variety of β-lactam antibiotics including third-generation cephalosporins and carbapenems. They have been classified into three groups according to their amino acid sequences. Subclass B1 is the largest and contains three well-studied β-lactamases: BcII from *Bacillus cereus* [2–4], CcrA from *Bacteroides fragilis* [5–8], and IMP-1 from *Pseudomonas aeruginosa* [9–11]. The subclass B2 prototypical enzyme is CphA from *Aeromonas hydrophila*, which strongly differs from other enzymes regarding zinc dependence and substrate profile [12]. Finally, subclass B3 contains the only tetrameric zinc β-lactamase described so far, the L1 enzyme from *Stenotrophomonas maltophilia* [13, 14], but tetramerization is not shared by all other members of this subclass [15].

The three-dimensional structures of BcII [2, 16], CcrA [5, 17, 18], IMP-1 [10], and L1 [14] have been solved, and they all show a similar αββα fold. Despite the overall structural similarity, some key residues, such as the zinc ligands or the residues involved in substrate binding, are not fully conserved, and this may explain some of the observed differences in substrate profiles. For subclass B1, all the structures available but one (obtained at low pH with BcII [19]) show the presence of two zinc ions in the active site. One zinc is coordinated by three histidines and a water molecule, which supposedly acts as the nucleophile during β-lactam hydrolysis. The second zinc ion is bound to a fourth histidine, an aspartate, a cysteine, and the nucleophilic water that forms a bridge between the two metals. An additional water molecule is usually bound to the second zinc and may serve as a proton donor during the catalytic process.

Recent findings concerning the catalytic mechanisms of both the mono- and di-zinc forms have been discussed elsewhere [20]. The rate-limiting step is often the opening of the β-lactam ring, and for the di-zinc form of the enzyme, two possible fates can be hypothesized for the tetrahedral intermediate. The first pathway (a in Figure 1A) is a concerted C-N cleavage occurring simultaneously with nitrogen protonation (the most probable proton donor being the water molecule bound to the second zinc). The second pathway (b in Figure 1A) derives from pre-steady-state studies performed in the presence of a chromogenic substrate, nitrocefin, suggesting that protonation of the lactam nitrogen prior to C-N cleavage is not required [8, 21, 22]. Instead, an intermediate with absorption maximum centered at 665 nm is transiently formed. This intermediate was identified by Wang and coworkers as the opened β-lactam with a negatively charged nitrogen stabilized by the second zinc ion [8]. Though attractive, this mechanism could be favored in the case of nitrocefin due to the possibility of charge delocalization and may not be a general feature of zinc β-lactamase catalysis.

X-ray structures obtained in the presence of inhibitors [10, 18, 23, 24] have suggested three main interaction sites between subclass B1 enzymes and their substrates [25]: (1) the lactam carbonyl probably interacts with the first zinc ion and the side chain of a well-conserved asparagine (N233 according to the standard numbering proposed recently [26]); (2) the substrate carboxylate may also be involved in interactions with the second zinc ion and the carbonyl of a peptide bond (belonging

*Correspondence: jmfrere@ulg.ac.be

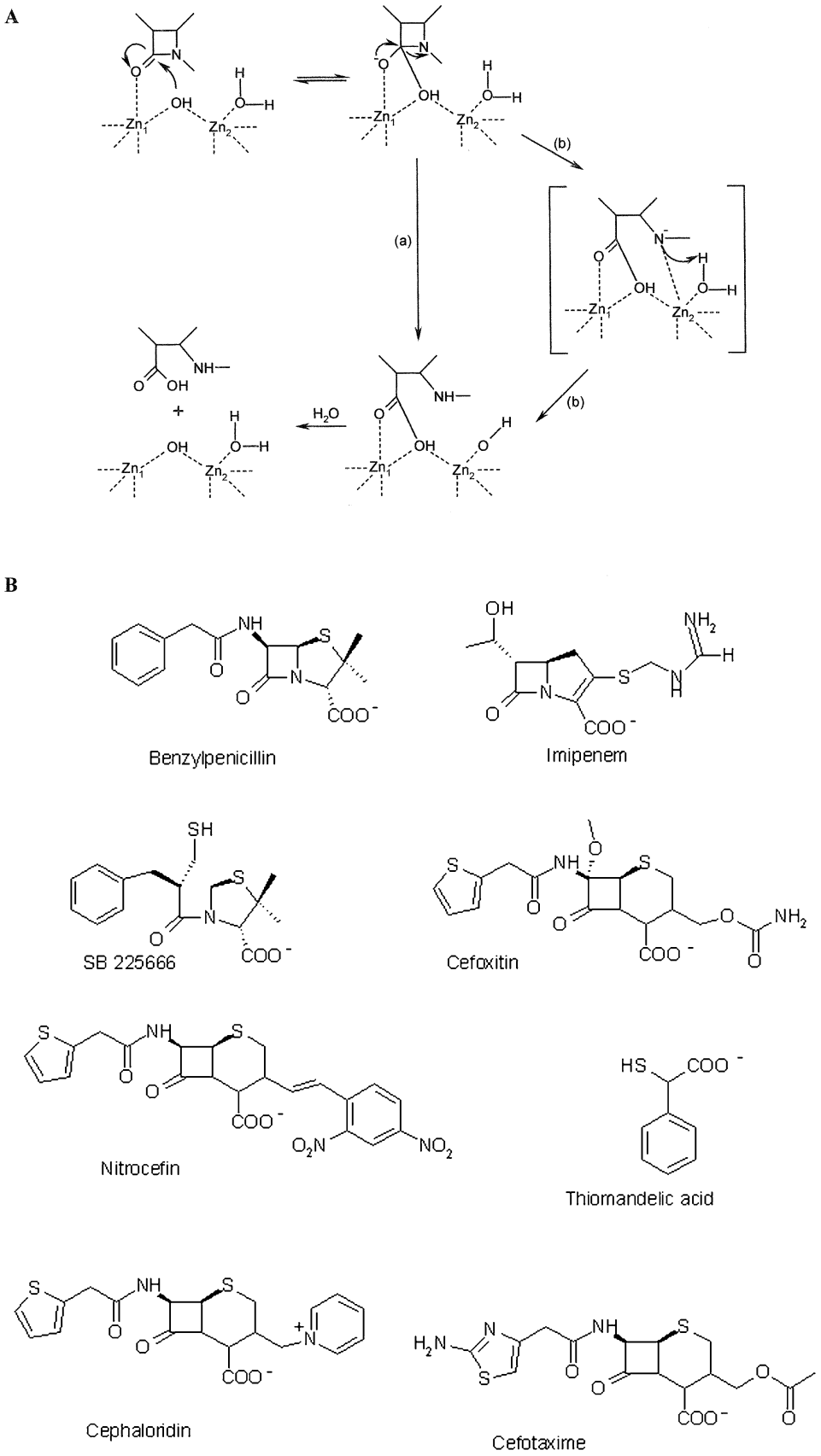

Figure 1. Possible Pathways for the Hydrolysis of β-Lactams by Metallo-β-Lactamases and Structures of the Compounds Used in the Present Study

(A) Possible pathways for the hydrolysis of β-lactams by metallo-β-lactamases.

(B) Structures of the compounds used in the present study.

to K224 or N233); (3) all β-lactamases whose three-dimensional structures are known contain a hydrophobic pocket likely to accommodate the C5/C6 substituents of substrates.

Recent studies have also pointed out that the flexible loop comprising residues 60–66 (standard numbering) in subclass B1 enzymes could be a major determinant for the tight binding of substrates and inhibitors in the active site. This loop is a typical feature of subclass B1 β-lactamases, but with the exception of a glycine residue at position 63, none of the residues in this loop are fully conserved (Figure 2). Nevertheless, the IMP-1 and CcrA β-lactamases share a common tryptophan residue (W64) whose position and flexibility is greatly modified upon inhibitor binding [10, 27–29]. The side chain of this tryptophan may serve as a lure to recruit hydrophobic substrates, triggering a large movement of the entire loop, which finally traps substrates into the active site [27, 29]. Deletion of the loop in the case of CcrA was shown to induce a severe loss of catalytic efficiency [7].

Here, we present a detailed study of the effect of the loop on substrate specificity and catalytic efficiency for two other main members of subclass B1 bearing distinct features, IMP-1 and BcII. The accumulation of the intermediate formed in the presence of nitrocefin is also shown to be affected by both the presence and the structure of the loop.

Results

Preliminary Characterizations of IMP-1 and BcII Mutants

Two mutants of IMP-1 were successfully prepared as confirmed by DNA sequence analysis and MS determination of protein molecular mass (Table 1). The first is a single amino acid substitution at position 64, where a tryptophan is found in the wild-type enzyme (W64A according to the standard numbering [26]), and the second results from the deletion of six residues ([61]VNGWGV[66]) in the wild-type enzyme (Δ61–66). The in vivo stability of IMP-1 was probably impaired in the absence of the loop, since the yield after purification dropped from approximately 20 mg/l for the wild-type and the W64A mutant to 3 mg/l for the Δ61–66 mutant. Nevertheless, after purification the protein was not obviously prone to degradation or denaturation, and the activity remained constant for several hours at 4°C. In agreement with these observations, comparison of the CD spectra for the three proteins did not reveal any

	57	70
BcII	ELGS	**FNGE.A**VPSN
IMP-1	SFEE	**VNGWGV**VPKH
CcrA	SLAE	**IEGWGM**VPSN
VIM-1/2	ATQS	**FDGA.V**YPSN
BlaB	TYNT	**FNGT.K**YAAN
IND-1	TFGV	**FGGK.E**YSAN

Figure 2. Sequence Alignments of the Active Site Loops in Subclass B1 Enzymes

Table 1. Molecular Mass, Zinc Content, and Kinetic Constants at 30°C for Various Substrates of IMP-1, W64A, and Δ61–66

	IMP-1			W64A			Δ61–66		
	K_m (μM)	k_{cat} (s^{-1})	k_{cat}/K_m (10^6 $M^{-1}s^{-1}$)	K_m (μM)	k_{cat} (s^{-1})	k_{cat}/K_m (10^6 $M^{-1}s^{-1}$)	K_m (μM)	k_{cat} (s^{-1})	k_{cat}/K_m (10^6 $M^{-1}s^{-1}$)
Benzylpenicillin	320 ± 50 (25)	200 ± 60 (94)	0.63 (3.8)	1250 ± 300	86 ± 11	0.07	>8500 (630)	>15 (1.5)	0.0017 (0.0024)
Nitrocefin	8.2 ± 1.4	130 ± 25	14	160 ± 8	700 ± 10	4.3	>1000	>900	2.7
Cephaloridin	5 ± 1.6 (12)	32 ± 5 (73)	6.4 (6.1)	>500	>250	0.31	>1300 (2700)	>19 (3.7)	0.015 (0.0014)
Cefotaxime	2.8 ± 0.2	13.4 ± 1.0	4.8	61 ± 2	98 ± 5	1.5	450 ± 7	129 ± 16	0.28
Cefoxitin	3.0 ± 1.1	9.0 ± 3.7	3.0	45 ± 1	40 ± 6	0.9	97 ± 14	8.6 ± 0.5	0.09
Imipenem	25 ± 2 (140)	68 ± 15 (74)	2.7 (0.52)	120 ± 12	67 ± 20	0.55	90 ± 25 (510)	100 ± 21 (1.8)	1.1 (0.0035)
Thiomandelic acid	0.030 ± 0.009[a]			0.060 ± 0.015[a]			0.136 ± 0.025[a]		
SB 225666	<0.44[a]			0.71 ± 0.022[a]			4.1 ± 1.0[a]		
Mr observed (calculated)	25,112 (25,113)			24,996 (24,998)			24,500 (24,499)		
[Zn]/[E]	1.7			1.9			1.8		

Mr values were obtained by electrospray mass spectrometry. SDs were ±5. Zinc content was determined by ICP/MS after dialysis against 10 mM HEPES (pH 7.5). The values are the means of two separate experiments with SDs close to 0.2. The kinetic parameters are the means of at least three separate experiments. The constants reported for CcrA3 and its Δ61–66 mutant are indicated in parentheses [7].
[a]Inhibition constant (K_i).

difference in the secondary and tertiary structures (data not shown). Determination of the amount of zinc bound to the wild-type and mutant enzymes by ICP/MS also demonstrated that the zinc content was only slightly affected by the alteration of the active site loop (Table 1), with an almost complete saturation of the two zinc binding sites in all cases.

Although the structure of the loop in IMP-1 and CcrA seems uniquely well adapted to promote tight ligand binding, a loop is also present in other subclass B1 enzymes. Interestingly, the BcII loop was recently shown to be directly involved in the binding of a mercaptocarboxylate inhibitor [30]. In order to compare the effect of the "BcII-like" loop with the better-known effect of the "CcrA-like" loop, we replaced the BcII loop (^{60}SFNGEA^{66}) with the IMP-1 loop (EVNGWGV). The loop ends were chosen on the basis of the three-dimensional structures of the unliganded enzymes in order to introduce minimum perturbations of the local environment. The resulting protein, named BcIIΔIMP, was unusually well expressed in the pET9a/BL21(DE3) system, with production yields reaching 150 mg/l after purification (compared to the 15–20 mg/l obtained with the wild-type). Finally, in order to compare the role of the tryptophan in the IMP-1 and BcII environments, W64A was mutated into an alanine in BcIIΔIMP, yielding BcIIΔIMP W64A. This last mutant was obtained with a yield of 48 mg/l. The Zn content indicated a complete saturation of the two binding sites for BcIIΔIMP and BcIIΔIMP W64A (Table 2).

Kinetic Parameters for the Wild-Type and Mutant Enzymes

Kinetic parameters for each mutant and corresponding wild-type enzyme were determined with the panel of substrates shown in Figure 1B.

Although the results (Tables 1 and 2) are analyzed in more detail in the Discussion, it can already be noted that the replacement of the loop tryptophan by an alanine results in an increase of the K_m values for all substrates in both the IMP-1 and the BcII backgrounds. With IMP-1, this mutation also increases the k_{cat} values for all cephalosporins, a result unprecedented in studies concerning the L1 loop of subclass B1 enzymes. In the BcII background, however, the effects of the W→A mutation on the turnover number are more diverse.

Effect of the Mutations on the Binding of Inhibitors

Two high-affinity inhibitors of different sizes (Figure 1B) were tested on the mutant enzymes. (*R*,*S*)-Thiomandelic acid is a simple mercaptocarboxylate compound that was shown to be a potent inhibitor of subclass B1 and B3 enzymes [30], while SB 225666 is a more complex inhibitor which binds to IMP-1 with high affinity [10]. Both inhibitors are zinc ligands, and their binding involves a large movement of the active site loop [10, 30].

Mutations of the IMP-1 loop resulted in a decreased affinity for both inhibitors, whereas introduction of the IMP-1 loop into BcII had a favorable effect (Tables 1 and 2). These data parallel the observed effects of the mutations on the K_m values described above, although the increases in K_i values were more moderate.

Table 2. Molecular Mass, Zinc Content, and Kinetic Constants at 30°C for Various Substrates of BcII, BcIIΔIMP, and BcIIΔIMP W64A

	BcII			BcIIΔIMP			BcIIΔIMP W64A		
	K_m (μM)	k_{cat} (s^{-1})	k_{cat}/K_m (10^6 $M^{-1}s^{-1}$)	K_m (μM)	k_{cat} (s^{-1})	k_{cat}/K_m (10^6 $M^{-1}s^{-1}$)	K_m (μM)	k_{cat} (s^{-1})	k_{cat}/K_m (10^6 $M^{-1}s^{-1}$)
Benzylpenicillin	150 ± 22	190 ± 50	1.2	32 ± 9	293 ± 4	9.2	154 ± 17	143 ± 6	0.9
Nitrocefin	10 ± 2	27 ± 7	2.7	5.2 ± 0.3	68 ± 9	13	11 ± 0.4	3.2 ± 0.1	0.3
Cephaloridin	>150[a]	>87[a]	0.30	47 ± 9	156 ± 30	3.3	560 ± 60	57 ± 4	0.1
Cefotaxime	24 ± 1	120 ± 30	5.0	7.0 ± 1.8	32 ± 7	4.6	38 ± 2	27 ± 1	0.7
Cefoxitin	240 ± 33	0.34 ± 0.01	0.0014	63 ± 4	0.35 ± 0.01	0.0055	930 ± 100	0.66 ± 0.04	0.0007
Imipenem	90 ± 12	117 ± 7	1.3	78 ± 4	104 ± 11	1.3	900 ± 90	180 ± 9	0.2
Thiomandelic acid	0.12 ± 0.02[b]			0.048 ± 0.007[b]			0.17 ± 0.02[b]		
SB 225666	1.62 ± 0.32[b]			0.40 ± 0.06[b]			1.5 ± 0.2[b]		
Hydrolyzed nitrocefin	780 ± 210[b]			420 ± 130[b]			685 ± 35[b]		
Mr observed (calculated)	24,957 (24,960)			25,098 (25,097)			24,983 (24,982)		
[Zn]/[E]	1.7			1.7			2.1		

Zinc content was determined by atomic absorption for BcII and BcIIΔIMP and by ICP/MS for the W64A mutant. Other conditions are as in Table 1.

[a] Substrate inhibition observed at high substrate concentrations.

[b] Inhibition constant (K_i).

Table 3. Kinetic Constants Obtained for BcII and BcIIΔIMP at 25°C

	BcII	BcIIΔIMP
k_1 ($M^{-1}s^{-1}$)	10^8	10^8
k_{-1} (s^{-1})	1100	730
k_2 (s^{-1})	23	108
k_3 (s^{-1})	920	678
k_4 ($M^{-1}s^{-1}$)	>1000	1000
$K = k_{-1}/k_1$ (μM)	11	7.3
K_m (μM) calcd/exp	11/10	6.6/5
k_{cat} (s^{-1}) calcd/exp	23/27	85/68

According to the model , $k_{cat} = k_2k_3k_4/(k_2k_3 + k_2k_4 + k_3k_4)$ and $K_m = k_{cat}(k_{-1} + k_2)/k_1k_2$. For the values of BcII, see text. For BcIIΔIMP, k_1 was not allowed to change. k_{-1}, k_2, k_3, and k_4 were constrained to be consistent with experimental K_m and k_{cat}, which are not significantly modified between 25°C and 30°C. A simulation performed with a fixed k_4 value of 10,000 did not yield a significantly different result.

Pre-Steady-State Study of the Mutants and Wild-Type Enzymes

The transient formation of an intermediate with an absorption maximum centered at 665 nm during hydrolysis of nitrocefin was demonstrated for two zinc β-lactamases (CcrA [8] and L1 [22]), suggesting that this may be a common feature of class B enzymes. A distinct intermediate with an absorption maximum around 450 nm was also described in the case of the BcII enzyme [31], but it could not be observed above −54°C. At present, no data are available at room temperature for this β-lactamase in the di-zinc form.

The wild-type enzymes and two of the mutants were studied under single turnover conditions (enzyme concentrations greater than substrate concentrations) with the help of a stopped-flow spectrophotometer at 25°C. The enzymes were rapidly mixed with nitrocefin at 25°C, and substrate depletion was monitored at 390 nm, product formation at 482 nm, and possible transient intermediate formation at 665 nm. No significant intermediate could be observed with wild-type BcII in the conditions of the experiment, but substrate depletion and product formation were easily followed. When increasing the substrate/enzyme ratio, the intermediate became observable and hydrolysis of 82 μM nitrocefin in the presence of 10 μM BcII (data not shown) led to the production of a maximum of 0.25 μM intermediate (0.3% of the initial substrate concentration and 2.5% of the enzyme). This shows that intermediate formation probably occurs at all substrate/enzyme ratios but remains below the detection limit when the substrate concentration is too low. Consequently, the minimum kinetic scheme accounting for the present observations is the linear model with one spectral intermediate EI,

$$E + S \rightleftarrows ES \rightarrow EI \rightarrow EP \rightleftarrows E + P,$$

where the last (k_4/k_{-4}) step reflects product inhibition (Table 3).

With BcIIΔIMP under the single turnover conditions, the presence of an intermediate absorbing at 665 nm was detected (Figure 3A). This suggested that the linear model is also valid for the BcII mutant. However, with an approximate dead time of 2.2 ms, it was impossible to record the rising phase of the curve, and only intermediate depletion could be observed. At the maximum of the curve, the intermediate accounted for 8% of the initial substrate concentration.

The time courses for BcII fitted a first-order equation reasonably well with a rate constant of 16 ± 1 s^{-1} for both the disappearance of substrate and the appearance of product. This could be explained on the basis of the linear model with a k_{-1}/k_1 value of 11 μM and a rate-limiting k_2 value of 23 s^{-1}. A k_3 value of about 920 s^{-1} would be needed to account for the 2.5% of intermediate formed at a saturating nitrocefin concentration. The value of k_4 cannot be approached in these experiments, since EP and P are expected to exhibit identical spectral properties at 482 nm. Product inhibition is irrelevant under single turnover conditions since product concentration never exceeded 5 μM, well below the K_i value (see Table 2). The experimental curves for BcIIΔIMP were simultaneously fitted with a program using the Matlab environment (see Experimental Procedures). The simulated curves are shown as thin, solid lines in Figure 3A, and the constants yielding the best fits are detailed in Table 3. When compared to the BcII values, the most striking feature is the increase of the k_2/k_3 ratio from 0.025 to 0.16, which accounts for the detection of the intermediate in the case of BcIIΔIMP. This is clearly more related to an increased k_2 than a decreased k_3 value. Product release (k_4) was again irrelevant since no modification of the calculated curves was observed upon increasing k_4 from 1,000 to 10,000 s^{-1}.

The pre-steady-state study of IMP-1 and W64A was more difficult because of higher k_{cat} values for nitrocefin. The use of a stopped-flow instrument with a lower dead time (1.6 ms) thermostatically controlled at 5°C instead of 25°C was necessary to obtain data points over a reasonable range of time (Figure 3B). Nevertheless, the quality and reproducibility of the recorded curves were insufficient to derive kinetic constants, and the curves were not further analyzed. Interestingly, however, the intermediate was observed only in the case of the wild-type IMP-1 (12% of the initial substrate concentration at the top of the recorded curve) and not for the W64A mutant. Evidence for intermediate formation was also obtained for W64A when the substrate/enzyme ratio was increased (data not shown), providing further support for the proposed kinetic scheme that seems to apply to a broad range of metallo-β-lactamases.

Discussion

The unusual degree of flexibility of the active site loop in subclass B1 metallo-β-lactamases was demonstrated by several authors [10, 14, 18, 23, 27, 30]. Scrofani et al. [27] suggested that the CcrA loop might be a major determinant of the broad specificity of this enzyme. Moreover, deletion of this loop was shown to be strongly detrimental to reaction rates and to the binding of substrates/inhibitors [7] (Table 1), suggesting that it directly influences catalysis. In the present work, we have deleted the IMP-1 loop that is similar to the CcrA loop (Figure 2) and introduced this loop in the *Bacillus cereus* metallo-β-lactamase. We also focused on residue W64,

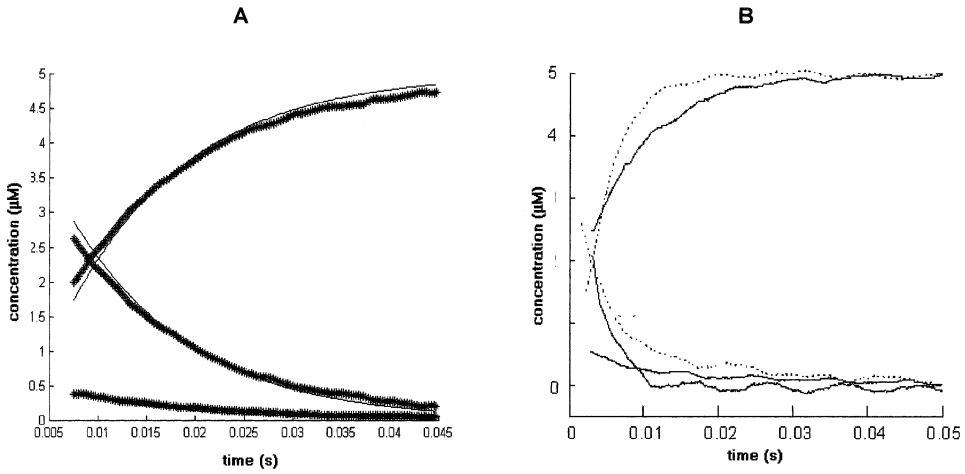

Figure 3. Time Courses for the Hydrolysis of Nitrocefin by BcIIΔIMP and by WT IMP-1 and Its W64A Mutant

(A) A solution of nitrocefin was rapidly mixed with BcIIΔIMP and buffer (final concentrations 5 μM and 25 μM, respectively) at 25°C (pH 7.5). Substrate depletion was monitored at 390 nm (decreasing curve from 5 μM), product formation at 482 nm (increasing curve), and intermediate formation at 665 nm (lowest curve) with the help of a stopped-flow spectrometer. Experimental (broader lines) and simulated (thinner lines) curves are shown. The 390 nm data were fitted as [S]+[ES], and the 482 nm data were fitted as [P]+[EP]. The values of the constants are those shown in Table 3.

(B) A solution of nitrocefin was rapidly mixed with IMP-1 (solid lines) or W46A (dashed lines) as in (A) but at 5°C. The wavelengths were as above.

whose influence was studied in the environment of both BcII and IMP-1.

The results obtained here with thiomandelic acid and SB 225666, which are both potent inhibitors of the wild-type enzymes, are consistent with the CcrA results [7, 27]: the best affinity is observed in the presence of the native IMP-1 loop, the W→A mutation is detrimental, and complete deletion of the loop even more so. Also in agreement with the present results is the structure of the IMP-1-SB 225666 complex [10], which highlights close contacts between the inhibitor and loop residues W64 and V67. Similarly, the NMR study of the BcII-thiomandelic acid complex [30] suggests that introduction of the IMP-1 loop into BcII might favor a hydrophobic interaction between the loop Trp residue and the inhibitor phenyl ring, an interaction which is lost in the W→A mutant of the hybrid. More unexpectedly, the K_i variations in the case of IMP-1 and BcII are far from being as spectacular as those observed in the case of CcrA. This is probably due to the fact that SB 225666 and thiomandelic acid both contain a thiol group and were shown to coordinate zinc ions. This interaction being certainly very strong can explain why the loss of potency observed upon loop deletion is rather moderate compared to what is observed with the penem used in the CcrA study (BRL 42715, which usually rather behaves as a substrate of metallo-β-lactamases [32]) or with the substrates used in the present study. Another possibility is that loop deletion induces more disorder in the protein scaffold of CcrA than in IMP-1.

The kinetic parameters of the various proteins with a set of substrates from various structural families (Figure 1B; penicillins, cephalosporins, cephamycins, and carbapenems) offer a more complex and informative picture. In agreement with the inhibition data, K_m values of all substrates are always increased when W64 is mutated to alanine in both BcII and IMP-1 backgrounds, and this increase is strengthened when the loop is completely deleted. However, K_m values represent combinations of microscopic rate constants, and their variations are more difficult to translate into terms of decreased/increased affinity than K_i values. In the particular case of nitrocefin, some clues are found in the pre-steady-state experiments. For this substrate with both BcII and BcIIΔIMP, k_{-1}/k_1 ratios are close to the K_m values (Table 3) and indicate that the latter parameters closely reflect the reversible binding of the substrate to the free enzyme. This might also be true for IMP-1 (if one assumes that intermediate concentration does not back extrapolate to a much higher value than the maximum reached in Figure 3B), since a relatively low level of intermediate accumulation is indicative of a low k_2 value. There are no experimental results showing that this is also the case for other substrates, but it is tempting to speculate that the major effect of W64 is to increase the affinity of substrates and inhibitors for the active site.

Although k_{cat} values are very diversely affected by loop modifications, it is quite clear that the structure of the IMP-1 loop globally benefits the enzymes since k_{cat}/K_m values are increased in all cases when the loop is present. However, in the IMP-1 environment the observed increases range from almost nothing for imipenem to around 400-fold for benzylpenicillin and cephaloridin. The latter value corresponds to $\Delta\Delta G^*$ of about 3.5 Kcal and indicates a rather strong influence of the loop on these two substrates. The direct consequence of these differential effects is a severe modification of the substrate specificity of IMP-1. To understand the molecular basis of the differences between substrates, it is interesting to examine the chemical structures of the studied compounds in relation with potential interaction sites.

As noted, benzylpenicillin is one of the substrates

most affected by tryptophan substitution and loop deletion. For this compound, increases in K_m are always associated with decreases in k_{cat}, resulting in severe losses of catalytic efficiencies. The same result had been obtained with the Δ61–66 mutant of CcrA (Table 1), which was shown to be 1500-fold less efficient than its wild-type counterpart [7]. Moreover, for this substrate, the effects of the W64A mutation in both IMP-1 and BcII backgrounds are strikingly similar. Recently reported docking experiments with benzylpenicillin and BcII [25] indicate that besides the so-called "oxyanion hole" and a loose interaction with K224, the active site loop contributes to substrate binding by providing hydrophobic interactions between the phenyl and methyl groups of benzylpenicillin and residues located at both ends of the loop (F61 and V67). Residues located at the top of the loop do not seem to be involved in substrate binding, but this model explains why complete deletion of the IMP-1 loop has a more drastic influence than simple substitution of the BcII loop with the IMP-1 loop. The latter replacement would probably conserve the interactions with V61 and V67 and supply additional ones with W64 that are lost in the W→A mutant. We performed a similar study with IMP-1 starting with the published coordinates [10]. It appeared that V61 also interacts with both methyl groups of benzylpenicillin, explaining why loop deletion is so detrimental to the interaction of this substrate with IMP-1 (V67 is still present but too far for productive interactions when residues 61–66 are deleted). The complete removal of the IMP-1 loop would thus eliminate a set of favorable interactions between the phenyl and methyl groups of benzylpenicllin and the side chains of V61, W64, and V67.

In the case of cephalosporins (nitrocefin, cephaloridin, and cefotaxime), the most unexpected result was the increase in k_{cat} values resulting from loop alterations. A similar result has been obtained with different mutants of the subclass B3 L1 metallo-β-lactamase [33]. For this protein, mutation of F158 or I164 belonging to another loop close to the active site (L2) also led to increased k_{cat} values with some of the tested substrates, namely cephalosporins and cefoxitin. However, the present kinetic data conflict with another report [7] showing that the turnover number of cephaloridin for the Δ61–66 mutant of CcrA was decreased 20-fold (Table 1). It also challenges the idea that the "CcrA loop" (found in CcrA and IMP-1) helps to lock the substrate into the active site and essentially facilitates the catalysis, as proposed previously by Huntley et al. [29]. Actually, cephalosporins are certainly well locked into the active site of IMP-1 (K_m values below 10 μM), but this could prevent the rapid transition to EI or EP that is required for optimum reaction rates. Thus, we propose that in some cases, depending on the particular topology of the considered enzyme and on the nature of the substrate, the loop forces the substrate into a position which is not the most favorable for nucleophilic attack, whereas in other cases the best relative positioning is found with the help of the loop. It is, however, premature to attempt a more detailed analysis of this phenomenon, since the two side chains of cephalosporins can potentially create numerous interactions with residues in the loop or elsewhere in the enzymes. To underline the influence of the enzyme background, one can note that the microscopic rate constants derived from the pre-steady-state study of nitrocefin with BcII and BcIIΔIMP indicate that in this particular case the IMP-1 loop has a modest effect on substrate affinity but significantly favors ES decay to EI, accounting for the detection of the intermediate with BcIIΔIMP. A similar situation could occur with IMP-1 and W64A, but the analysis is complicated by the fact that the single turnover experiment with the latter was performed at a substrate concentration well below the K_m value, a reason which is sufficient to explain the absence of intermediate.

Actually, Fast et al. [34] had already predicted from the study of the C121R mutant of the *B. fragilis* enzyme, whose characteristics are similar to those of BcII, at least with the studied substrates, that C-N bond cleavage (k_2) might be rate limiting in the case of nitrocefin and BcII in contrast to CcrA and L1. The present data confirm this hypothesis and additionally show that the short-range environment of the zinc is not the only crucial factor in increasing catalytic efficiency. Here, we demonstrate that modification of the loop, which in the free protein is relatively far from the catalytic site, can also lead to significant accelerations of C-N bond cleavage and turnover number, at least in the case of BcII and when nitrocefin is the substrate.

The turnover number of cefoxitin is only moderately affected by loop modifications in IMP-1 and BcII. Consequently, changes in K_m values are likely to be more directly related to changes in substrate binding capacity, which makes cefoxitin a good model compound for molecular modeling. Figure 4 shows that when cefoxitin is positioned in the IMP-1 active site in a global orientation similar to that of benzylpenicillin, the Oγ of serine 121 is well oriented to interact with the methoxy group of the cephamycin. However, no obvious interaction seems to be possible between the active site loop and the substrate. Molecular dynamics was used to test the possibility that other stable conformers of the IMP-1 loop exist; interestingly, two other stable orientations of the loop were found that are close to each other but more distant from the initial loop. In these conformers, the global orientation of the loop is moderately affected (the W64 Cα atoms are shifted by 2.8 Å), but the side chain of W64 is strongly displaced (a 4.5 Å movement of W64 Nε is observed). In this orientation also, W64 comes closer to cefoxitin, and its Nε1 can make a hydrogen bond with the carbonyl of the substrate C3 side chain. From the experimental data presented in Tables 1 and 2, it is likely that for cefoxitin, S121 and W64 account for most of the interaction energy. When they are absent (BcII), cefoxitin becomes a very poor substrate.

The case of the carbapenem compound, imipenem, is one of the most intriguing in this study. Actually, its kinetic parameters are barely affected by the presence or amino acid composition of the active site loop. In Table 1, the largest difference between the $k_{ca}t/K_m$ values of IMP-1 and the W64A mutant corresponds to a $\Delta\Delta G^*$ value of less than 1 Kcal/mol, and the single residue mutation is more detrimental than complete loop removal. The reported data on loop deletion with CcrA [7] also indicated that the loss of catalytic efficiency was

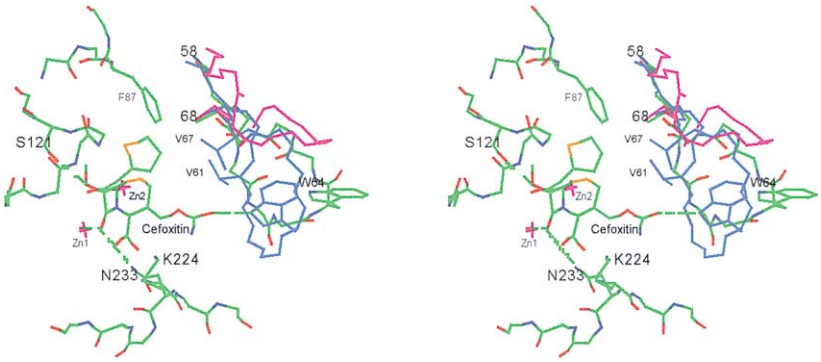

Figure 4. Proposed Interactions between Cefoxitin and the IMP-1 β-Lactamase

The loop of the free enzyme is color coded. The loop resulting from the molecular dynamics calculations is in cyan (only one conformer is represented), and the BcII loop is in purple. Both ends of the loops are marked (58, 68). The interactions (see text) are shown as dashed lines.

at least one order of magnitude lower than that observed with benzylpenicillin and cephaloridin (Table 1), although the k_{cat} value decreased 40-fold (while it was unaffected with IMP-1). Being that the most clinically relevant property of metallo-β-lactamases is their capacity to efficiently hydrolyze carbapenems, this result certainly requires further interpretation. The most obvious explanation refers to the polar nature of the imipenem side chain (the terminal amidine function is positively charged at neutral pH), which probably precludes stable interactions with the loop. The positive charge by itself is not detrimental since cephaloridin also bears a charged nitrogen, but the absence, in imipenem, of the cephaloridin aromatic pyridinium group might prevent the former from interacting with the tryptophan. The model presented in Figure 4 for cefoxitin also suggests that imipenem might develop a stabilizing interaction involving its hydroxyl group and S121. That this interaction prevails over interactions with the loop in the case of IMP-1 would be an interesting hypothesis for future mutagenesis. Similarly, in BcII and in other enzymes devoid of W64 like the VIM-type enzymes [35], mechanisms should also exist to compensate for the absence of interactions with the loop. Even if the C_6 or C_7 side chains of penicillins or cephalosporins, respectively, are often hydrophobic, the data presented here with imipenem restrict the scope of the previous proposition that the mobile loop is a major determinant for the broad substrate recruitment of class B1 enzymes [27]. Clearly, other mechanisms must operate in the case of imipenem. This is underlined by the fact that if the W64A mutation increases the K_m values in both the BcII and IMP-1 backgrounds, the K_m value of CcrA (140 μM) is larger than that of the IMP-1 mutant, where the loop has been completey deleted (90 μM), and that both very low (1.5 and 9 μM for VIM-1 and VIM-2, respectively) and rather high (360 μM for BlaB) K_m values can be observed in the absence of tryptophan in the loop. Similarly, k_{cat}/K_m values for imipenem differ by a factor of 30 between the two members of the VIM family, which share identical loops but exhibit mutations in several other positions [35].

To conclude about the well-characterized mobility of W64 in CcrA and IMP-1 [27, 29, 10] and the marked trends observed here upon loop modification and deletion, substrate binding in most cases seems to occur along the following lines. First, even in the absence of crystallographic data for enzyme-substrate complexes, two active site residues have been predicted to play a major role in substrate binding: K224 and N233. However, mutational analyses of their influence in various class B enzymes [7, 36, 37] demonstrate that they are not essential for binding or catalysis. In the absence of evidence for other interaction sites, substrate binding seems to proceed through a set of rather loose interactions, and significant stabilization is expected to occur upon closing of the active site by the mobile loop. Second, substrate binding is also facilitated by the variety of conformations that can be adopted by the tryptophan located at the top of the loop, contributing to create a very plastic cavity. This plasticity orientates substrate specificity but is not the only mechanism at the origin of the broad substrate profile of class B enzymes. Indeed, BcII, the VIM enzymes, and IMP-1 can hydrolyze the same substrates even if their catalytic efficiencies are not identical, and IMP-1, CcrA, BlaB, BcII, VIM-1, and VIM-2 all exhibit low K_m values for nitrocefin, ranging from 8 to 20 μM, whether the loop contains a tryptophan or not. Finally, other residues in the loop (like hydrophobic residues at positions 61 and 67) certainly develop interactions with substrates side chains as exemplified by the BcII loop. Interestingly, this loop mechanism could be common to subclass B1 and B3 enzymes since mutants of an active site loop in L1 were shown to induce similar modifications of kinetic parameters [33].

Significance

Our study demonstrates that a loop which is relatively far from the active site in the free enzyme significantly affects ligand binding and turnover numbers. It also highlights some residues which probably play a prominent role in the loop. Based on the kinetic data obtained in the IMP-1 background, W64 seems to account for approximately 50% of the loop effect, since all the trends observed for Km and k_{cat}/Km with W64A become enhanced around 2-fold upon loop deletion. Our data are in agreement with previous interpretations of the unusual mobility of W64 [27, 29], suggesting that it mainly contributes to create a plastic active site capable of binding a large variety of molecules with high affinity, probably through hydrophobic interactions. Interestingly, substrates with a weak hydrophobic character, such as imipenem, are not excluded from the substrate profile of subclass B1 enzymes, showing that this loop effect is not a necessary

mechanism for efficient hydrolysis, at least in the presence of other anchoring points (for instance, S121 in the IMP-1-imipenem interaction). According to molecular modeling, residues 61 and 67, located at the base of the loop, seem to play an important role beyond their hinge function. Finally, we showed that the loop-induced increased affinity is imperfectly correlated with high turnover numbers, showing the limits of the "plastic strategy" developed by subclass B1 enzymes. The total effect measured in terms of k_{cat}/K_m clearly identifies the loop as a useful tool for metallo-β-lactamases, but it is certainly not the only one and can even be insignificant in the interaction between some enzymes and imipenem.

Experimental Procedures

Materials

Oligonucleotides were synthesized by Pharmacia. Restriction enzymes, T4 ligase, and T4 kinase were from Promega and Invitrogen. Chloramphenicol, cephaloridine (ϵ^{260} = 12,000 $M^{-1}cm^{-1}$; $\Delta\epsilon^{260}$ = −10,000 $M^{-1}cm^{-1}$), cefoxitin (ϵ^{260} = 8250 $M^{-1}cm^{-1}$; $\Delta\epsilon^{260}$ = −6600 $M^{-1}cm^{-1}$), and cefotaxime (ϵ^{260} = 16,000 $M^{-1}cm^{-1}$; $\Delta\epsilon^{260}$ = −7500 $M^{-1}cm^{-1}$) were purchased from Sigma. Kanamycin was obtained from Merck, benzylpenicillin (ϵ^{235} = 1250 $M^{-1}cm^{-1}$; $\Delta\epsilon^{235}$ = −775 $M^{-1}cm^{-1}$) from Aventis, imipenem (ϵ^{300} = 9000 $M^{-1}cm^{-1}$; $\Delta\epsilon^{300}$ = −9000 $M^{-1}cm^{-1}$) from Merck Sharp & Dohme, and nitrocefin (ϵ^{390} = 19,500 $M^{-1}cm^{-1}$; $\Delta\epsilon^{482}$ = 17,500 $M^{-1}cm^{-1}$) from Unipath Oxoid. Bovine serum albumin (BSA) was from Boehringer Mannheim. Thiomandelic acid was synthesized as described [30], and SB 225 666 was a generous gift of SmithKline Beecham Pharmaceuticals.

Site-Directed Mutagenesis

The QuickChange Site-Directed Mutagenesis kit from Stratagene was used for all PCR amplifications. For the W64A mutant of IMP-1 (W64A), two sets of overlapping primers were used to amplify the pET9a plasmid bearing the entire bla_{IMP} gene (including signal peptide; the modified bases are underlined): 5′-TTGAAGAAGTTAACGG GGCGGGCGTTGTTCCTAAACA-3′ and 5′-TGTTTAGGAACAACG CCCGCCCCGTTAACTTCTTCAA-3′. Deletion of residues 61–66 in IMP-1 (Δ61–66) was achieved with two 30-base primers corresponding to residues preceding (first primer) and following (second primer) those deleted: 5′-TTCTTCAAACGAAGTATGAACATAAACGCC-3′ and 5′-GTTCCTAAACATGGTTTGGTGGTTCTTGTA-3′. For BcIIΔIMP, the pBluescript plasmid containing the BcII gene devoid of a signal peptide was used for PCR amplification with two partially overlapping primers that contained floating 5′ ends corresponding to the seven introduced IMP-1 residues (underlined): 5′-GAAGTTAACGG GTGGGGCGTTGTTCCTTCGAACGGTCTAGTTCTTAAT-3′ and 5′-AAC GCCCCACCCGTTAACTTCACCTAACTCCGTATGAACCCATACATT-3′. The NdeI/BamHI 800 bp fragment was subcloned into the pET9a vector. Finally, the W64A mutant of BcIIΔIMP (BcIIΔIMP W64A) was obtained like the W64A mutant of IMP-1, starting with pET9a bearing the $bla_{BcII\Delta IMP}$ gene and two sets of overlapping primers: 5′-GGTGAA GTTAACGGGGCGGGCGTTGTTCCTTCG-3′ and 5′-CGAAGGAACA ACGCCCGCCCCGTTAACTTCACC-3′. After transformation in *E. coli* DH5α cells, the sequences of all mutants were checked for introduction of the desired mutations and absence of unwanted ones.

Enzyme Production and Purification

Wild-type IMP-1, BcII, and the various mutants were produced in *E. coli* BL21 (DE3) and purified according to described procedures [9, 36]. After concentration and dialysis, the purified enzymes were stored at −20°C. For BcIIΔIMP, an additional step was necessary to remove a dark violet pigment, and enzyme samples were dialyzed overnight against 100 mM citrate (pH 5.4) and then against three changes of 50 mM HEPES (pH 7.5) containing 1 mM $ZnSO_4$. Protein concentrations were determined using the BCA assay (Pierce) and the absorbance at 280 nm (ϵ = 44,600 $M^{-1}cm^{-1}$ for IMP-1; 38,900 $M^{-1}cm^{-1}$ for W64A and Δ61–66; 30,500 $M^{-1}cm^{-1}$ for BcII; 34,850 $M^{-1}cm^{-1}$ for BcIIΔIMP; 29,160 $M^{-1}cm^{-1}$ for BcIIΔIMP W64A).

Circular Dichroism

Conservation of secondary and tertiary structures was checked by circular dichroism with a Jobin-Yvon CD6 instrument purged with a nitrogen flow. Enzymes were diluted to 0.2 mg/ml in a phosphate buffer (5 mM, pH 7.5), and the temperature was set at 25°C. Five spectra were acquired between 190 and 250 nm (far UV CD; 0.1 cm path length cell) or between 250 and 360 nm (near UV CD; 1 cm path length cell) and averaged.

Mass Spectrometry

The *Mr* of the wild-type and mutant enzymes was estimated using an electrospray mass spectrometer as described [15].

Determination of Zinc Content

The zinc content of the enzymes was determined by ICP/MS at the Institut Malvoz de la Province de Liège (Liège, Belgium). For BcII and BcIIΔIMP, atomic absorption was used in the flame mode, and experiments were performed on a Perkin Elmer 2100 spectrometer. Prior to the experiment, enzyme samples were dialyzed against 10 mM HEPES (pH 7.5), and protein concentrations were measured at 280 nm.

Enzyme Kinetics and Inhibition Studies

Hydrolysis of the antibiotics by wild-type and mutant enzymes was followed by monitoring the variations of absorbance at the appropriate wavelength. Experiments were performed with a Uvikon XL (Bio-Tek Instruments) spectrophotometer equipped with thermostatically controlled cells (30°C). The reactions were conducted in 10 mM HEPES (pH 7.5) in a total volume of 500 μl, and BSA was added to the diluted enzyme solutions (final concentration, 20 μg/ml). The steady-state kinetic parameters were determined by fitting the initial rates with the Henri-Michaelis equation or by analyzing the complete time courses as described by De Meester et al. [38]. When low K_m values were obtained (<5 μM), they were confirmed by substrate competition using nitrocefin as a reporter substrate. When the K_m values were too large to be estimated, the k_{cat}/K_m ratio was derived from the analysis of the complete time course at low substrate concentrations (below the K_m). Finally, inhibition constants (K_i) were obtained with nitrocefin (thiomandelic acid) or imipenem (SB 225666) as a reporter substrate, assuming a competitive pattern of inhibition and plotting, $v_0/v_i = f([I])$, where v_0 is the initial rate in the absence of inhibitor, and v_i is the initial rate in the presence of inhibitor. The slope of the resulting line is $K_m/((K_m + [S]).K_i)$. With SB 225666, inhibition was usually slow, except for Δ61–66 and BcII. For W64A, BcIIΔIMP, and BcIIΔIMP W64A, v_i were determined between 2.5 and 3 min and fitted to the equation above. For IMP-1, inhibition reached the steady state only after 7 min, and at this stage a non-negligible amount of substrate had already been hydrolyzed, compromising the determination of an accurate K_i value. Finally, hydrolyzed nitrocefin was prepared as follows: a 3 mM solution of nitrocefin in 50 mM phosphate buffer (pH 8.0) was hydrolyzed by 0.6 nmol of BcIIΔIMP for 15 min at 30°C and filtered on an Ultrafree-15 Centrifugal Filter Device (Millipore). The concentration of the filtrate was determined spectrophotometrically (ϵ^{390} = 7000 $M^{-1}cm^{-1}$), and inhibition constants were determined as described above with imipenem as substrate.

Stopped-Flow Experiments

These were carried out in 50 mM HEPES (pH 7.5) at 5 or 25°C on a UV-visible spectrometer equipped with a Bio-Logic SFM-3 or SFM-4 stopped-flow unit and a 1 cm path length cell. The data were recorded on a personal computer and stored with the Biokine software delivered with the instrument. In a typical experiment, a solution of enzyme (containing a 1.5-fold excess of BSA w/w to reduce enzyme adhesion to the cell walls) was rapidly mixed with nitrocefin and buffer, and a minimum of three reproducible experiments were averaged. Nitrocefin was dissolved at a 0.1 M concentration in dimethyl formamide and diluted to the desired concentration with buffer. Substrate depletion was monitored at 390 nm ($\Delta\epsilon$ = −12 500 $M^{-1}cm^{-1}$), product formation at 482 nm ($\Delta\epsilon$ = 17,500 $M^{-1}cm^{-1}$), and intermediate formation and decay at 665 nm (ϵ = 31,000 $M^{-1}cm^{-1}$ based on previously published reports [8, 22]). Each set of data was corrected for the theoretical instrument dead time (2.2 ms for the

Bio-Logic SFM-3 instrument and 1.6 ms for the Bio-Logic SFM-4 instrument). The data obtained with WT BcII were fitted to the first-order equations with the help of the K_i routine [38]. Those obtained with the BcIIΔIMP mutant were fitted to the linear kinetic mechanism with one spectral intermediate (EI) within the Matlab software environment (version 5.3, MathWorks Inc.). The routine uses the *lsqcurvefit* function, which solves nonlinear least squares problems. The differential equations of the model are solved by a low-order Runge-Kutta method (*ode23* function) that only needs to know the solution at the preceeding point. The value of k_1 was set to the diffusion limit (10^8 $M^{-1}s^{-1}$), k_2 and k_3 were varied, and k_{-1} was adjusted accordingly to be consistent with the experimental values of K_m and k_{cat}. The value of k_4 successively set to 1,000, 2,000, and 10,000 did not influence the result.

Docking Experiments and Molecular Dynamics

Docking experiments were run as described in a previous paper [25]. To perform molecular dynamics, the coordinates of all atoms were fixed to their values in the IMP-1 β-lactamase structure ([10]; PDB ID code 1DD6), except those of residues 59 to 69 limiting the loop. These atoms were allowed to move in a very simple molecular dynamics run consisting of a 40 ps equilibration run and a 40 ps production run with a time step of 1 fs. The calculations were performed using Discover (Molecular Simulations, San Diego, CA) and the CVFF force field.

Acknowledgments

We thank Marc Jamin, Bernard Sartor, and Yves Dupont (CEA, Grenoble, France) for welcoming us in their laboratory to perform some of the stopped-flow experiments and Annabelle Lejeune for helpful discussions. This work was supported by European research networks on zinc β-lactamases (ERB-FMRX-CT-98-0232 and HPRN-CT-2002-00264) and by the Belgian program Pôles d'Attraction Interuniversitaire (PAI P5/33). C.A. is supported by a Marie Curie Fellowship.

Received: January 16, 2002
Revised: February 4, 2003
Accepted: March 13, 2003
Published: April 21, 2003

References

1. Kuwabara, S., and Abraham, E.P. (1967). Some properties of two extracellular beta-lactamases from Bacillus cereus 569/H. Biochem. J. *103*, 27C–30C.
2. Fabiane, S.M., Sohi, M.K., Wan, T., Payne, D.J., Bateson, J.H., Mitchell, T., and Sutton, B.J. (1998). Crystal structure of the zinc-dependent beta-lactamase from Bacillus cereus at 1.9 A resolution: binuclear active site with features of a mononuclear enzyme. Biochemistry *37*, 12404–12411.
3. Orellano, E.G., Girardini, J.E., Cricco, J.A., Ceccarelli, E.A., and Vila, A.J. (1998). Spectroscopic characterization of a binuclear metal site in Bacillus cereus beta-lactamase II. Biochemistry *37*, 10173–10180.
4. Paul-Soto, R., Bauer, R., Frère, J.M., Galleni, M., Meyer-Klaucke, W., Nolting, H., Rossolini, G.M., de Seny, D., Hernandez-Valladares, M., Zeppezauer, M., et al. (1999). Mono- and binuclear Zn2+-beta-lactamase. Role of the conserved cysteine in the catalytic mechanism. J. Biol. Chem. *274*, 13242–13249.
5. Concha, N.O., Rasmussen, B.A., Bush, K., and Herzberg, O. (1996). Crystal structure of the wide-spectrum binuclear zinc beta-lactamase from Bacteroides fragilis. Structure *4*, 823–836.
6. Paul-Soto, R., Hernadez-Valladares, M., Galleni, M., Bauer, R., Zeppezauer, M., Frère, J.M., and Adolph, H.W. (1998). Mono- and binuclear Zn-beta-lactamase from Bacteroides fragilis: catalytic and structural roles of the zinc ions. FEBS Lett. *438*, 137–140.
7. Yang, Y., Keeney, D., Tang, X., Canfield, N., and Rasmussen, B.A. (1999). Kinetic properties and metal content of the metallo-beta-lactamase CcrA harboring selective amino acid substitutions. J. Biol. Chem. *274*, 15706–15711.
8. Wang, Z., Fast, W., and Benkovic, S.J. (1999). On the mechanism of the metallo-beta-lactamase from Bacteroides fragilis. Biochemistry *38*, 10013–10023.
9. Laraki, N., Franceschini, N., Rossolini, G.M., Santucci, P., Meunier, C., de Pauw, E., Amicosante, G., Frère, J.M., and Galleni, M. (1999). Biochemical characterization of the Pseudomonas aeruginosa 101/1477 metallo-beta-lactamase IMP-1 produced by Escherichia coli. Antimicrob. Agents Chemother. *43*, 902–906.
10. Concha, N.O., Janson, C.A., Rowling, P., Pearson, S., Cheever, C.A., Clarke, B.P., Lewis, C., Galleni, M., Frère, J.M., Payne, D.J., et al. (2000). Crystal structure of the IMP-1 metallo beta-lactamase from Pseudomonas aeruginosa and its complex with a mercaptocarboxylate inhibitor: binding determinants of a potent, broad-spectrum inhibitor. Biochemistry *39*, 4288–4298.
11. Haruta, S., Yamaguchi, H., Yamamoto, E.T., Eriguchi, Y., Nukaga, M., O'Hara, K., and Sawai, T. (2000). Functional analysis of the active site of a metallo-beta-lactamase proliferating in Japan. Antimicrob. Agents Chemother. *44*, 2304–2309.
12. Hernandez Valladares, M., Felici, A., Weber, G., Adolph, H.W., Zeppezauer, M., Rossolini, G.M., Amicosante, G., Frère, J.M., and Galleni, M. (1997). Zn(II) dependence of the Aeromonas hydrophila AE036 metallo-beta-lactamase activity and stability. Biochemistry *36*, 11534–11541.
13. Crowder, M.W., Walsh, T.R., Banovic, L., Pettit, M., and Spencer, J. (1998). Overexpression, purification, and characterization of the cloned metallo-beta-lactamase L1 from Stenotrophomonas maltophilia. Antimicrob. Agents Chemother. *42*, 921–926.
14. Ullah, J.H., Walsh, T.R., Taylor, I.A., Emery, D.C., Verma, C.S., Gamblin, S.J., and Spencer, J. (1998). The crystal structure of the L1 metallo-beta-lactamase from Stenotrophomonas maltophilia at 1.7 A resolution. J. Mol. Biol. *284*, 125–136.
15. Mercuri, P.S., Bouillenne, F., Boschi, L., Lamotte-Brasseur, J., Amicosante, G., Devreese, B., van Beeumen, J., Frère, J.M., Rossolini, G.M., and Galleni, M. (2001). Biochemical characterization of the FEZ-1 metallo-beta-lactamase of Legionella gormanii ATCC 33297(T) produced in Escherichia coli. Antimicrob. Agents Chemother. *45*, 1254–1262.
16. Carfi, A., Duee, E., Paul-Soto, R., Galleni, M., Frère, J.M., and Dideberg, O. (1998). X-ray structure of the ZnII beta-lactamase from Bacteroides fragilis in an orthorhombic crystal form. Acta Crystallogr. D Biol. Crystallogr. *54*, 45–57.
17. Carfi, A., Duee, E., Galleni, M., Frère, J.M., and Dideberg, O. (1998). 1.85 Å resolution structure of the zinc (II) beta-lactamase from Bacillus cereus. Acta Crystallogr. D Biol. Crystallogr. *54*, 313–323.
18. Fitzgerald, P.M., Wu, J.K., and Toney, J.H. (1998). Unanticipated inhibition of the metallo-beta-lactamase from Bacteroides fragilis by 4-morpholineethanesulfonic acid (MES): a crystallographic study at 1.85-Å resolution. Biochemistry *37*, 6791–6800.
19. Carfi, A., Pares, S., Duee, E., Galleni, M., Duez, C., Frère, J.M., and Dideberg, O. (1995). The 3-D structure of a zinc metallo-beta-lactamase from Bacillus cereus reveals a new type of protein fold. EMBO J. *14*, 4914–4921.
20. Wang, Z., Fast, W., Valentine, A.M., and Benkovic, S.J. (1999). Metallo-beta-lactamase: structure and mechanism. Curr. Opin. Chem. Biol. *3*, 614–622.
21. Wang, Z., Fast, W., and Benkovic, S.J. (1998). Direct observation of an enzyme bound intermediate in the catalytic cycle of the metallo-beta-lactamase from Bacteroides fragilis. J. Am. Chem. Soc. *120*, 10788–10789.
22. McManus-Munoz, S., and Crowder, M.W. (1999). Kinetic mechanism of metallo-beta-lactamase L1 from Stenotrophomonas maltophilia. Biochemistry *38*, 1547–1553.
23. Toney, J.H., Fitzgerald, P.M., Grover-Sharma, N., Olson, S.H., May, W.J., Sundelof, J.G., Vanderwall, D.E., Cleary, K.A., Grant, S.K., Wu, J.K., et al. (1998). Antibiotic sensitization using biphenyl tetrazoles as potent inhibitors of Bacteroides fragilis metallo-beta-lactamase. Chem. Biol. *5*, 185–196.
24. Toney, J.H., Hammond, G.G., Fitzgerald, P.M., Sharma, N., Balkovec, J.M., Rouen, G.P., Olson, S.H., Hammond, M.L., Greenlee, M.L., and Gao, Y.D. (2001). Succinic acids as potent inhibitors of plasmid-borne IMP-1 metallo-beta-lactamase. J. Biol. Chem. *276*, 31913–31918.

25. Prosperi-Meys, C., Wouters, J., Galleni, M., and Lamotte-Brasseur, J. (2001). Substrate binding and catalytic mechanism of class B beta-lactamases: a molecular modelling study. Cell. Mol. Life Sci. *58*, 2136–2143.
26. Galleni, M., Lamotte-Brasseur, J., Rossolini, G.M., Spencer, J., Dideberg, O., and Frère, J.M. (2001). Standard numbering scheme for class B beta-lactamases. Antimicrob. Agents Chemother. *45*, 660–663.
27. Scrofani, S.D., Chung, J., Huntley, J.J., Benkovic, S.J., Wright, P.E., and Dyson, H.J. (1999). NMR characterization of the metallo-beta-lactamase from bacteroides fragilis and its interaction with a tight-binding inhibitor: role of an active-site loop. Biochemistry *38*, 14507–14514.
28. Salsbury, F.R., Jr., Crowley, M.F., and Brooks, C.L., 3rd. (2001). Modeling of the metallo-beta-lactamase from B. fragilis: structural and dynamic effects of inhibitor binding. Proteins *44*, 448–459.
29. Huntley, J.J., Scrofani, S.D., Osborne, M.J., Wright, P.E., and Dyson, H.J. (2000). Dynamics of the metallo-beta-lactamase from Bacteroides fragilis in the presence and absence of a tight-binding inhibitor. Biochemistry *39*, 13356–13364.
30. Mollard, C., Moali, C., Papamicael, C., Damblon, C., Vessilier, S., Amicosante, G., Schofield, C.J., Galleni, M., Frère, J.M., and Roberts, G.C. (2001). Thiomandelic acid, a broad spectrum inhibitor of zinc beta-lactamases: kinetic and spectroscopic studies. J. Biol. Chem. *276*, 45015–45023.
31. Bicknell, R., and Waley, S.G. (1985). Cryoenzymology of Bacillus cereus beta-lactamase II. Biochemistry *24*, 6876–6887.
32. Matagne, A., Ledent, P., Monnaie, D., Felici, A., Jamin, M., Raquet, X., Galleni, M., Klein, D., François, I., and Frère, J.-M. (1995). Kinetic study of interaction between BRL 42715, β-lactamases, and D-Alanyl-D-Alanine peptidases. Antimicrob. Agents Chemother. *39*, 227–231.
33. Carenbauer, A.L., Garrity, J.D., Periyannan, G., Yates, R.B., and Crowder, M.W. (2002). Probing substrate binding to metallo-β-lactamase L1 from Stenotrophomonas maltophilia by using site-directed mutagenesis. BMC Biochem. *3*, 4.
34. Fast, W., Wang, Z., and Benkovic, S.J. (2001). Familial mutations and zinc stoichiometry determine the rate-limiting step of nitrocefin hydrolysis by metallo-beta-lactamase from Bacteroides fragilis. Biochemistry *40*, 1640–1650.
35. Docquier, J.D., Lamotte-Brasseur, J., Galleni, M., Amicosante, G., Frère, J.-M., and Rossolini, G.M. (2003). On functional and structural heterogeneity of VIM-type metallo-β-lactamases. J. Antimicrob. Chemother. *51*, 257–266.
36. de Seny, D., Prosperi-Meys, C., Bebrone, C., Rossolini, G.M., Page, M.I., Noel, P., Frère, J.M., and Galleni, M. (2002). Mutational analysis of the two zinc binding sites of the Bacillus cereus 569/H/9 metallo-beta-lactamase. Biochem. J. *363*, 687–696.
37. Haruta, S., Yamamoto, E., Eriguchi, Y., and Sawai, T. (2001). Characterization of the active-site residues asparagine 167 and lysine 161 in the IMP-1 metallo beta-lacatamase. FEMS Microbiol. Lett. *197*, 85–89.
38. De Meester, F., Joris, B., Reckinger, G., Bellefroid-Bourgignon, C., and Frère, J.M. (1987). Automated analysis of enzyme inactivation phenomena: Application to beta-lactamases and DD-peptidases. Biochem. Pharmacol. *36*, 2393–2403.